Direct Observation of Ballistic Electrons in Silicon Dioxide

D. J. DiMaria, M. V. Fischetti, J. Batey, L. Dori,[a] E. Tierney, and J. Stasiak
IBM Thomas J. Watson Research Center, Yorktown Heights, New York 10598
(Received 26 August 1986)

Vacuum-emission and carrier-separation techniques have been used to make the first direct observation of ballistic electron transport in silicon dioxide, and the first direct observation in any material of the interaction of ballistic electrons with single phonons of the lattice. With very thin oxides, total ballistic transport of the electrons is observed for voltages of $\lesssim 1$ V dropped across the remaining oxide portion after tunneling. For voltage drops >1 V, a transition from the ballistic to the steady-state regime is seen. Monte Carlo simulations are used to predict the observed experimental behavior including quantum-mechanical interference effects and phonon-induced sidebands in the electron distributions.

PACS numbers: 72.20.Fr

Ballistic electron transport in GaAs and InGaAs semiconductors is currently receiving much attention.[1-5] Three terminal layered structures composed of GaAs (Ref. 1), GaAs/GaAlAs (Refs. 2 and 3), or InGaAs/InAlAs (Ref. 4) were used to energy analyze hot electrons. For the best reported case, *direct* observation of ballistic transport of up to 75% of the injected distribution was seen.[3] However, because of the electron-electron interactions in the heavily doped base regions of these devices, single phonon scattering events of ballistic electrons cannot be observed.

In an earlier time period (1975), ballistic electron transport in amorphous SiO_2 (a wide-bandgap insulator) was originally claimed by Lewicki and Maserjian. This was based on the observation of oscillations in current-voltage data for very thin layers (30–75 Å) of SiO_2.[6] In 1984, similar oscillations were reported in III-V structures by Hickmott *et al.*[7] Although indirect, these observations first suggested the existence of ballistic electrons in these materials.

Recently, transport in SiO_2 has been reevaluated both experimentally[8-12] and theoretically.[13-18] These studies showed that significant electron heating occurs in SiO_2 under fields as low as 1.5–2 MV/cm (Refs. 11–14). The mean free path length was determined theoretically to vary between 8 and 15 Å depending on the electric field magnitude.[16] After runaway of the electron distribution from the dominant energy loss of the longitudinal-optical (LO) phonon modes at 0.153 and 0.063 eV, a steady-state condition is reached after an energy gain of ≈ 3 eV (with respect to the bottom of the SiO_2 conduction band) for an electric field magnitude of ≈ 4 MV/cm (Refs. 9, 11, 14, and 16). Stabilization is believed to be achieved by the additional *large-angle* acoustic and band-edge phonon scattering which occurs at these energies and increases the actual path length traversed by the electrons.[14,16] However, LO-phonon emission is still the dominant energy-loss mechanism. Electron heat-up or cool-down distances to a steady-state condition and energy-relaxation distances once in steady state for the entire electron distribution are on the order of 20–30 Å (Refs. 9 and 16).

Within the current framework for electron transport in SiO_2, *very thin* oxide layers should show current-voltage oscillations due to quantum interference, provided that the interface of the oxide with the contacting electrode is abrupt. The magnitude of the oscillations should reflect the percentage of hot carriers in the distribution that are ballistic and have not been scattered. The purpose of this Letter is to report the first *direct* measurement of ballistic transport in SiO_2 with use of the carrier-separation and vacuum-emission techniques.[8-12] Additionally, we report the first direct observation in any material of single-phonon scattering, of ballistic electrons. These data are also compared with Monte Carlo calculations that include the quantum interference effects, over the full range of oxide thicknesses and voltages for ballistic behavior.

The experimental techniques and device structures used in these studies have been described in previous publications[8-12] and will only briefly be reviewed here. Vacuum emission directly measures the hot-electron distribution ejected into vacuum. These few emitted electrons (≈ 1 in 10^5–10^6) that are not scattered by the metal gate electrode are believed to be characteristic of the hot-electron distribution in SiO_2 as it enters the metal anode.[10] Information can be gained about both the average energy of the hot electrons, and the energy distribution itself. Carrier separation, which requires *p*-channel field-effect transistors (FET's), only measures the average energy of the distribution.[9] This is done by counting the number of electron-hole pairs produced in a crystalline silicon substrate by the incoming hot SiO_2 conduction-band electrons and by use of a sufficiently realistic theory[19] to convert this number to an average energy. The main advantage of the carrier-separation technique over the vacuum-emission technique is that it counts *all* the incoming electrons since scattering by a thin metal overlayer does not occur. With use of both techniques, a consistent picture of electron heating

without any assumptions can be formed.

The devices used for the vacuum-emission experiments consisted of large area (~ 0.01 cm^2) metal-oxide semiconductor structures with thin SiO_2 layers of thickness t_{ox}, ranging from 40 to 100 Å. Both low-temperature (350 °C) plasma-enhanced chemical-vapor deposition[20] and high-temperature (850 °C) thermal oxidation[21] were used to form the oxide layers. The data from the plasma-enhanced chemical-vapor deposition SiO_2 films were indistinguishable from the thermally grown layers. Both single metallizations using thin Al (120–250 Å) or double metallizations employing Au (200–250 Å)/Al (200–250 Å) on top of the SiO_2 layer were used in the vacuum-emission experiments.[10,12] Only electron energies $\gtrsim 0.9$ eV could be studied in these experiments.

The devices used for the carrier-separation studies were p-channel FET's with thin (37–66 Å) thermally grown SiO_2 layers. As described in previous studies, these devices had small gate areas ($\leq 10^{-4}$ cm^2) formed from polycrystalline silicon (poly-Si) which was degenerately doped n type with phosphorus.[9,12]

Figure 1 shows the data for average energy ($\langle E \rangle$) as a function of the voltage dropped across the remaining portion of oxide after tunneling (ΔV) for $\Delta V \leq 2$ V. As depicted in the energy band inset in Fig. 1, $\Delta V \equiv V_{ox} - \Phi_B/e$ where V_{ox} is the voltage dropped across the SiO_2 layer, e is the magnitude of the charge on an electron, and Φ_B is the interfacial barrier height ($\simeq 3.1$ eV). Positive values of ΔV imply Fowler-Nordheim tunneling from a metal or silicon contact to the bottom of the oxide conduction band as illustrated, while negative values imply direct tunneling from metal or silicon contact to the opposite metal or silicon contact. In this figure, carrier-separation data are compared to Monte Carlo simulations which include quantum interference effects that will be discussed later. For the oxide thickness range studied here between 37 and 66 Å, this figure shows reasonable agreement between theory and experiment with ballistic transport for most electrons occurring below 1 V. Ballistic transport by definition implies no energy loss of the electrons by inelastic scattering phenomena as they traverse the SiO_2 layer; that is, $\langle E \rangle \equiv e\Delta V$ which is illustrated in Fig. 1 by the solid line.

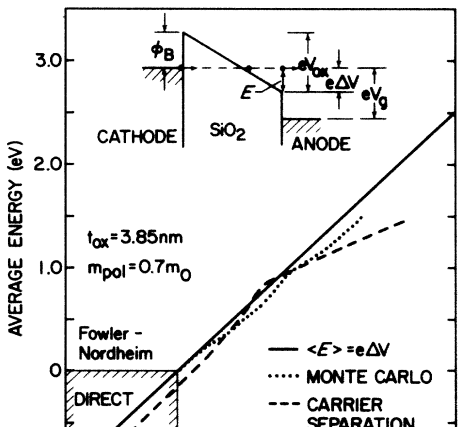

FIG. 1. Comparison of experiment and theory at room temperature for ballistic electron transport in a 38.5-Å-thick SiO_2 layer. Average electron energy (defined with respect to the bottom of the SiO_2 conduction band) is shown as a function of the remaining voltage dropped across the oxide layer after tunneling. For the carrier-separation experiments, data from several devices with varying gate areas and geometries were used. The solid line represents the ballistic condition as shown in the energy-band diagram which illustrates the voltage drops of interest.

The undulations in the data and simulations of Fig. 1 are believed to be due to quantum-mechanical interference effects. These oscillations are clearly visible in the Fowler-Nordheim tunneling current, as shown in Fig. 2. The period of the oscillation is strongly dependent on the oxide thickness. The amplitude depends on the fraction of electrons which ballistically reach the anode. In Fig. 2, we compare the experimental data from FET's similar to those used in the carrier-separation studies of Fig. 1 with the results of a conventional Monte Carlo simulation. The experimental data shown are for ballistic electrons impinging on the crystalline-Si-substrate/SiO_2 interface after tunnel injection from the poly-Si gate electrode. Since both Si interfaces with the SiO_2 layer are abrupt in the FET's, identical data were obtained for the other voltage polarity where ballistic electrons impinged on the poly-Si gate. Thus, the effect of the density of

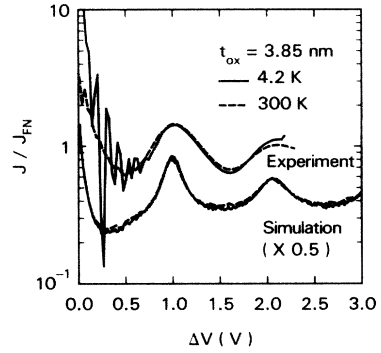

FIG. 2. Ratio of the observed tunneling current density J to the WKB expression J_{FN} (see Ref. 6) at two different temperatures, showing the oscillations due to the quantum reflections at the Si/SiO_2 interface. The simulations are obtained by integrating the Schrödinger equation and by accounting for the electron–LO-phonon scattering in the SiO_2 conduction band. The very weak temperature dependence is due to the high energy of the dominant LO-phonon modes. Data and the Monte Carlo simulations are shifted from each other by a factor of 2 for visualization.

states for the anode material (expected to cause broadening when tunneling into the randomly oriented crystalline grains of the poly-Si gate) appears to have little if any connection with these oscillations. Other gate materials, such as metals like Al, Cr, Ni, Mg, etc., which react with SiO_2 do not show the pronounced oscillations seen with Si.

The Monte Carlo calculations were performed by variation of the polaron-corrected effective mass of the electron (m_{pol}) to fit the amplitude of the current oscillations. The best fit was found for $m_{pol}=0.7m_0$, where m_0 is the free-electron mass. This value is in good agreement with the value of $0.68m_0$ which can be obtained from first-order perturbation theory following Ref. 16 (footnote 54) and accounting for the two LO phonons. The mean free path deduced from this simulation is $\simeq 13$ Å for the range of fields and oxide thicknesses used here, consistent with the previous studies of Lewicki and Maserjian.[6]

Figure 3 shows the average energy as a function of the voltage drop for transport in the transition from the ballistic to the steady-state regime. In the steady-state regime, the distance traversed is large enough that most of the carriers in the electron distribution have been stabilized by acoustic and band-edge phonon scattering. In this figure, vacuum-emission data are displayed in addition to the carrier-separation data and the Monte Carlo calculations. Given the experimental differences between the two techniques and some of the assumptions in the calculations the overall agreement is reasonable. In particular, the nonpolar scattering rates used in the simulation are uncertain for electron energies in the range from 1 to 2 eV.[16] The data of Figs. 1 and 3 indicate that in this range the scattering rate is slightly higher than the first-order rates used in the Monte Carlo simulation, as suggested by higher-order calculations.[17] Again undulations, believed to be due to the quantum interference effects are experimentally observed (particularly, in the carrier-separation data) as predicted by the simulations. The discrepancy between the vacuum-emission and carrier-separation data could be due to scattering effects of the polycrystalline-Al-metal gate and/or the Al/SiO_2 interface in the vacuum-emission experiments.

Figure 4 shows the electron-energy distribution determined from the vacuum-emission data in the near ballistic regime and compares it to a Monte Carlo simulation. The peak in the simulation at 1.12 eV is due to the ballistic electrons while the other peaks are sidebands created by LO-phonon emission for energies <1.12 eV or by LO-phonon absorption for energies >1.12 eV. These peaks appear at integral multiples of the LO-phonon energies of 0.063 and 0.153 eV. (This is the first time single-phonon scattering of ballistic electrons has been observed in any material.) Additional structure arises from the combinations of the two modes. As steady state is approached at higher voltages and/or for thicker oxides, most of this structure due to phonon scattering of some of the ballistic electrons disappears in both the Monte Carlo calculations and in the data. On thinner oxides, the ballistic peak becomes more pronounced relative to the phonon-induced sidebands, until on the thinnest SiO_2 layers studied it dominates the spectrum.

The authors wish to acknowledge the device preparation by the IBM Thomas J. Watson Research Center and the Raleigh, North Carolina, silicon processing facil-

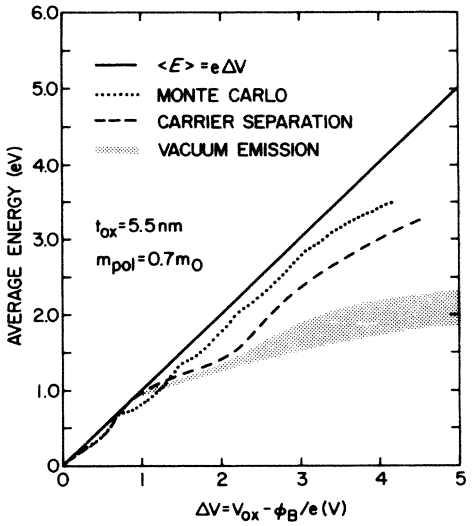

FIG. 3. Comparison of experiment and theory at room temperature for the transition from ballistic to steady-state transport in 55-Å-thick SiO_2 layers. Notation is the same as in Fig. 1. Vacuum-emission data, shown by the cross-hatched area, include structures with oxide thickness varying from 53 to 102 Å.

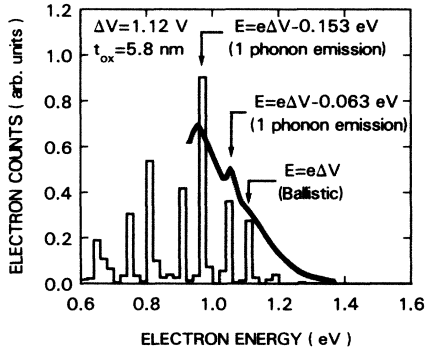

FIG. 4. Experimental (heavy curve) and simulated (solid line) energy distribution of the electrons in a very thin (58 Å) oxide at room temperature. The experimental curve is obtained by calculation of the derivative of the total number of electron counts vs analyzer voltage in the vacuum-emission experiment (see Ref. 10).

ities; the assistance of T. N. Theis in the use of his computer program for the analysis of the carrier-separation data; and the critical reading of this manuscript by F. Stern.

---

[a]Permanent address: Laboratorio dei Materiali per l'Elettronica (LAMEL), I-40126 Bologna, Italy.

[1]A. F. J. Levi, J. R. Hayes, P. M. Platzman, and W. Weigmann, Phys. Rev. Lett. **55**, 2071 (1985).

[2]M. Heiblum, M. I. Nathan, D. C. Thomas, and C. M. Knoedler, Phys. Rev. Lett. **55**, 2200 (1985).

[3]M. Heiblum, I. M. Anderson, and C. M. Knoedler, Appl. Phys. Lett. **49**, 207 (1986).

[4]U. K. Reddy, J. Chen, C. K. Peng, and H. Morkoc, Appl. Phys. Lett. **48**, 1799 (1986).

[5]N. Yokoyama, K. Imamura, T. Ohshima, H. Nishi, S. Muto, K. Kondo, and S. Hiyamizu, *IEDM Technical Digest 1984* (IEEE, San Francisco, 1984), pp. 532–534.

[6]G. Lewicki and J. Maserjian, J. Appl. Phys. **46**, 3032 (1975).

[7]T. W. Hickmott, P. M. Solomon, R. Fischer, and H. Markoç, Appl. Phys. Lett. **44**, 90 (1984).

[8]T. N. Theis, D. J. DiMaria, J. R. Kirtley, and D. W. Dong, Phys. Rev. Lett. **52**, 1445 (1984).

[9]D. J. DiMaria, T. N. Theis, J. R. Kirtley, F. L. Pesavento, D. W. Dong, and S. D. Brorson, J. Appl. Phys. **57**, 1214 (1985).

[10]S. D. Brorson, D. J. DiMaria, M. V. Fischetti, F. L. Pesavento, P. M. Solomon, and D. W. Dong, J. Appl. Phys. **58**, 1302 (1985).

[11]D. J. DiMaria, M. V. Fischetti, E. Tierney, and S. D. Brorson, Phys. Rev. Lett. **56**, 1284 (1986).

[12]D. J. DiMaria, M. V. Fsichetti, M. Arienzo, and E. Tierney, J. Appl. Phys. **60**, 1719 (1986).

[13]H. H. Fitting and J. U. Frieman, Phys. Status Solidi (a) **69**, 349 (1982).

[14]M. V. Fischetti, Phys. Rev. Lett. **53**, 1755 (1984).

[15]W. Porod and D. K. Ferry, Phys. Rev. Lett. **54**, 1189 (1985).

[16]M. V. Fischetti, D. J. DiMaria, S. D. Brorson, T. N. Theis, and J. R. Kirtley, Phys. Rev. B **31**, 8124 (1985).

[17]M. V. Fischetti and D. J. DiMaria, Phys. Rev. Lett. **55**, 2475 (1985).

[18]W. Porod and D. K. Ferry, in Proceedings of the Fourth International Conference on Hot Electrons in Semiconductors, Innsbruck, Austria, 1985, edited by E. Gornik, Physica B (Amsterdam) (to be published).

[19]R. C. Alig, S. Bloom, and C. W. Struck, Phys. Rev. B **22**, 5565 (1980).

[20]J. Batey and E. Tierney, J. Appl. Phys. **60**, 3136 (1986).

[21]M. Arienzo, L. Dori, and T. N. Szabo, unpublished.

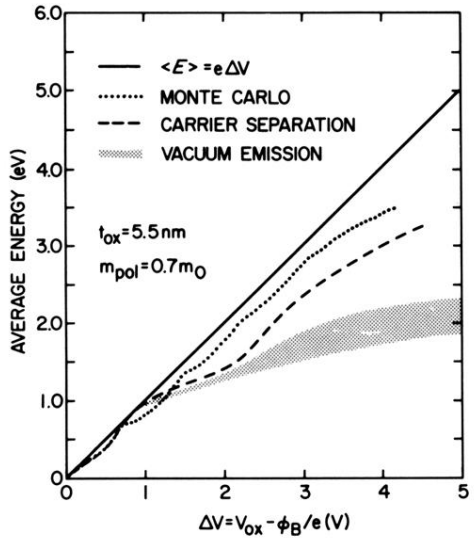

FIG. 3. Comparison of experiment and theory at room temperature for the transition from ballistic to steady-state transport in 55-Å-thick SiO_2 layers. Notation is the same as in Fig. 1. Vacuum-emission data, shown by the cross-hatched area, include structures with oxide thickness varying from 53 to 102 Å.